

# Effect of Wall Material on H<sup>-</sup> Production in a Plasma Sputter-Type Ion Source

**Y. D. M. Ponce\*, J. R. S. Lazarte, and H. J. Ramos**

Plasma Physics Laboratory,  
National Institute of Physics, University of the Philippines,  
Diliman, Quezon City 1001  
E-mail: dponce@nip.upd.edu.ph

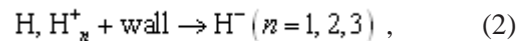
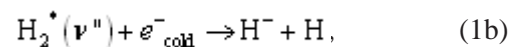
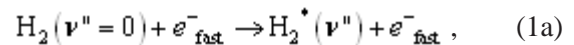
## ABSTRACT

The effect of wall material on negative hydrogen ion (H<sup>-</sup>) production was investigated in a multicusp plasma sputter-type ion source (PSTIS). Steady-state cesium-seeded hydrogen plasma was generated by a tungsten filament, while H<sup>-</sup> was produced through surface production using a molybdenum sputter target. Plasma parameters and H<sup>-</sup> yields were determined from Langmuir probe and Faraday cup measurements, respectively. At an input hydrogen pressure of 1.2 mTorr and optimum plasma discharge parameters  $V_d = -90$  V and  $I_d = -2.25$  A, the plasma parameters  $n_e$  was highest and  $T_e$  was lowest as determined from Langmuir probe measurements. At these conditions, aluminum generates the highest ion current density of 0.01697 mA/cm<sup>2</sup>, which is 64% more than the 0.01085 mA/cm<sup>2</sup> that stainless steel produces. The yield of copper, meanwhile, falls between the two materials at 0.01164 mA/cm<sup>2</sup>. The beam is maximum at  $V_f = -125$  V. Focusing is achieved at  $V_L = -70$  V for stainless steel,  $V_f = -60$  V for aluminum, and  $V_f = -50$  V for copper. The results demonstrate that proper selection of wall material can greatly enhance the H<sup>-</sup> production of the PSTIS.

## INTRODUCTION

Negative ion beams are extensively used in several fields including nuclear fusion and high-energy physics (Nishiura et al., 1998). Such beams are generally produced with three types of sources: volume, surface, and hybrid sources. The plasma sputter-type ion source (PSTIS) in the Plasma Physics Laboratory designed by Ramos (1995) for thin-film formation via ion beam deposition is distinctly of the surface conversion type due to the presence of a Mo converter electrode, which, when biased negatively with respect to the chamber wall (anode), causes the ions to self-extract towards the beam diagnostic chamber for beam analysis. Aside from the surface production mechanism occurring in

the converter surface, H<sup>-</sup> can also be generated from the plasma bulk by a dissociative attachment process and along the walls as described in Eqs. (1) and (2), respectively:



where

$\text{H}_2(v''=0)$  = hydrogen molecule in ground state,  
 $\text{H}_2^*(v'')$  = highly rovibrationally excited H<sub>2</sub> molecule,  
 $e_{\text{fast}}^-$  = fast or high-energy electron, and  
 $e_{\text{cold}}^-$  = cold or low-energy electron.

For practical applications like thin-film deposition, the ion beam must have high negative ion current output.

\*Corresponding author

However, in a previous study conducted on the same device, the extracted  $H^-$  current ( $\sim 0.097$  nA) was very minimal (Ranay, 2002). Several optimization and enhancement procedures have been performed on the extracted beam including argon-mixing (Ubarro, 2003), beam focusing (Yambot, 1999), and Cs seeding, which so far has proven to be the most effective with the highest  $H^-$  yield of 33.1 nA (Yambot, 2003).

Another possible technique that has considerable effect on the production rate of ions is the modification of the wall material of the ion source by installing various metal liners. Leung et al. (1985) investigated the effect of different metal liners on the chamber wall of a magnetically filtered multicusp source. For the specific device used, the differences in current yield were attributed to the amount of secondary electrons emitted from the wall surfaces. The presence of secondary electrons of energies  $\gg 8$  eV reduced the  $H^-$  yield considerably.

The relatively low yield of stainless steel indicates that the walls of the all-stainless-steel ion source of the PSTIS pose an inherent limitation to the production of  $H^-$  beams. Hence in the study, the effect of varying the wall material of the ion source on the  $H^-$  yield was carried out to resolve this limitation.

## EXPERIMENT

The facility utilized in this experiment, the PSTIS, is shown schematically Fig. 1. Hydrogen plasma is produced within the ion source chamber made up of

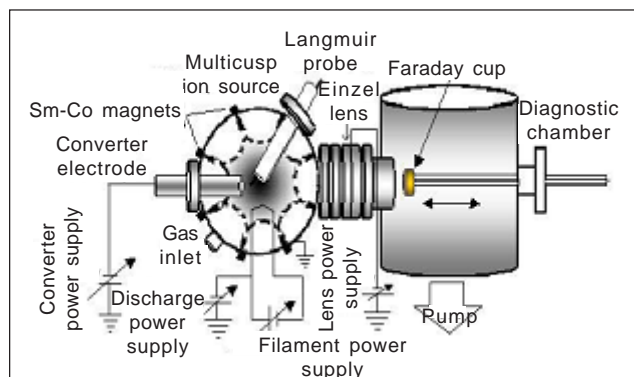


Fig. 1. Schematic diagram of the PSTIS.

an all-stainless-steel cylinder measuring 10.8 cm in diameter and 14 cm in length, with an approximate volume of one liter. Eight columns of Sm-Co magnets surround the cylinder, while the side flanges each have six columns forming a multicusp magnetic configuration for plasma confinement, reducing the loss of primary electrons and thereby increasing the plasma density.  $H^-$  are produced through surface production using a Mo converter (concave disc with 10 cm focal length, 1.5 cm thickness, and 2.4 cm diameter), while thermionic emission from a tungsten filament (0.05 cm diameter and 9 cm length) provides the primary electrons. Al and Cu metal liners with thickness of 0.28 mm were used as substitutes to the purely stainless steel ion source chamber to be able to study the effect of varying the wall material in the production of negative ions. Plasma characteristics are obtained by the Langmuir probe, while the  $H^-$  current is measured by a Faraday cup.

The effect of altering the wall material on plasma parameters was investigated in a pure and a cesiated-hydrogen discharge at 1.2 mTorr input hydrogen pressure in a vacuum system with a base pressure of  $10^{-6}$  Torr.

## RESULTS AND DISCUSSION

Prior to  $H^-$  beam extraction, plasma characteristics were determined to establish the optimum plasma conditions for the production of  $H^-$ . The conditions of the plasma influence  $H^-$  production and destruction. Langmuir probe measurements yield the pertinent parameters: electron temperature  $T_e$  and electron density  $n_e$  from the  $I-V$  curve of the plasma.  $T_e$  and  $n_e$  are indicators of the rate of formation, destruction, and extraction of  $H^-$  ions in a surface production multicusp source (Uramoto, 1985). Higher  $n_e$  and lower  $T_e$  are positive conditions for the formation of negative ions.  $T_e$  describes the energy of the electrons present in the plasma. Low  $T_e$  coupled with high  $n_e$  point to the presence of more slow or cold electrons, necessary for the formation of  $H^-$  from an excited molecular hydrogen  $H_2(v')$  by dissociative electron attachment (Wengrow et al., 1998). Electrons of high energies, called “hot” electrons, tend to destroy the already formed  $H^-$  within the bulk of the plasma.

Shown in Figs. 2 and 3 are the  $T_e$  and  $n_e$  at varying discharge current  $I_d$ .

From Fig. 2, the electron temperature generally decreases with increasing discharge current. Such behavior is attributed to the increased electron-ion and electron-neutral interactions at higher  $I_d$  due to shorter mean free paths of the particles, offsetting the initial energies of the electrons.  $n_e$  on the other hand, exhibits a converse behavior; that is,  $n_e$  increases with  $I_d$  as illustrated in Fig. 3. This trend agrees with expected results since the number of electrons per unit time is increased with increasing  $I_d$ .

Addition of Cs vapor further reduced  $T_e$  and increased  $n_e$ . Hence, it is expected that the ion yield from the cesiated plasma would be much higher than that of the uncesiated case. The increase in the ion yield can be accounted from the following underlying mechanisms (Fukumasa et al., 1996): electron cooling (i.e., lower  $T_e$ ), production of  $H_2(v''')$  due to reaction between Cs atoms and  $H_3^+$ ,  $H^-$  surface production caused by H

atoms and positive hydrogen ions and lowering of the work function of the surface material.

Similar behaviors of  $T_e$  and  $n_e$  are observed for the three materials, both for the cesiated and uncesiated cases. The value of  $n_e$  peaks at  $I_d = -2.25$  A and at the same time,  $T_e$  has a low value at this condition. Thus, the discharge condition most suitable for beam characterization is at  $I_d = -2.25$  A and  $V_d = -90$  V.

It is also notable from the plots that among the three wall materials, the plasma with highest  $n_e$  and lowest  $T_e$  is produced with the Al liner, most defined upon addition of Cs, followed by the Cu liner, and the stainless steel obtained the lowest. This behavior is due to the dependence of  $n_e$  on the work function of the metals used. Lower work function means easy removal of electrons from the boundary of the metal, thereby increasing the presence of more low-energy electrons in the plasma upon bombardment of primary electrons into the chamber walls. Results for the uncesiated case, on the other hand, are inconclusive due to overlapping values obtained. Hence only the cesiated case is considered in the characterization of the  $H^-$  beam.

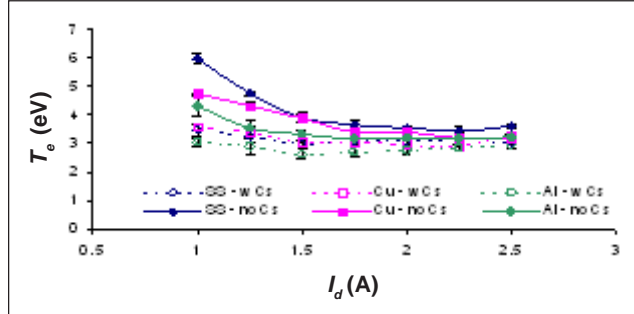


Fig. 2. Comparison of  $T_e$  and  $I_d$  for stainless steel, Al, and Cu metal liners in pure and Cs-seeded H plasma at  $V_t = 0$ .

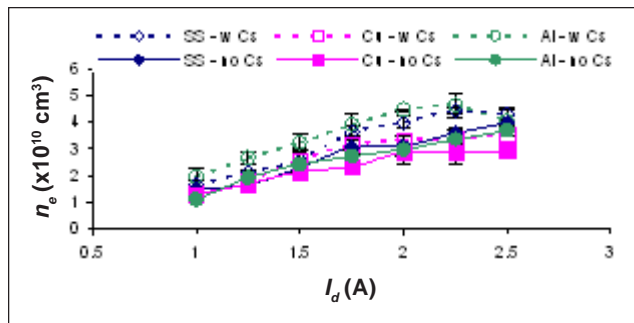


Fig. 3. Comparison of  $T_e$  and  $I_d$  in pure and Cs-seeded H plasma at  $V_t = 0$ .

Upon determination of the optimum  $n_e$  and  $T_e$ , optimization of the target potential  $V_t$  was carried out. Results show that the  $H^-$  current values produced by the three wall materials increase with  $V_t$ , consistently peak at  $-125$  V, and then gradually decrease thereafter as depicted in Fig. 4.

The target potential determines the energy of the ions leaving the surface of the Mo target. Thus, increasing  $V_t$  is expected to increase the energies of the  $H^-$  ions repelled towards the diagnostic chamber, leading to an increased number of  $H^-$  with enough energy to reach the detector, hence, the greater  $H^-$  current with increasing  $V_t$ . The subsequent diminishing values of  $H^-$  current density at  $V_t$  greater (more negative) than  $-125$  V may seem anomalous. However, this may be accounted for by the secondary electron emission at the collector of the Faraday cup upon impact of the negative ions. The Faraday cup is made of brass, which is 60%–80% copper. Copper begins to emit secondary electrons when hit by particles of energies approaching 200 eV (Weast, 1986). Hence, at higher target potentials these electrons may reduce the detected current. At

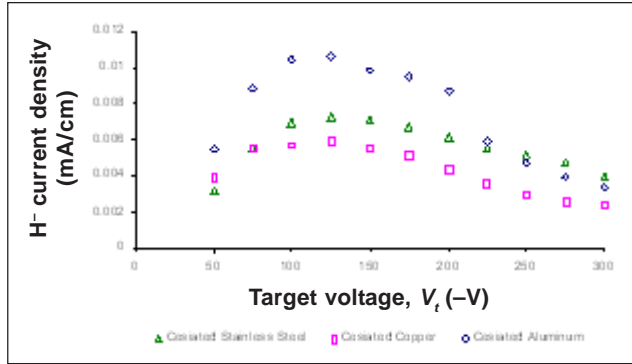


Fig. 4. Optimization of the Mo target potential. The  $H^-$  current density peaks at  $V_t = -125$  V.

optimum  $V_t = -125$  V, the extracted  $H^-$  current densities are 0.0106, 0.00592, and 0.00730 mA/cm<sup>2</sup> for Al, Cu, and stainless steel (SS), respectively.

The high current density values detected for the cesiated case, even without focusing of the beam, are three orders of magnitude higher than the previously optimized uncesiated results (Ranay, 2002). Even when compared with the previous results obtained with cesium-seeded hydrogen plasma (Yambot, 2003), the difference is approximately two orders of magnitude higher. This is attributed to the difference in the operating temperature of the cesium oven (180°C compared with 300°C in previous experimental runs). Overcoverage of cesium on the surface of the Mo converter is known to cause a diminishing of  $H^-$  yield. For the present case, the high  $H^-$  current suggests that no destructive effect occurred in the production of ions due to excessive amount of cesium (Wengrow et al., 1998).

At optimum target voltage,  $V_t = -125$  V, the input voltage to the Einzel lens is varied from 0 V to -150 V. Figure 5 clearly describes the effect of  $V_L$  on the detected current. The current density generally increases until the optimal value of  $V_L$  is achieved. Focusing of the beam with the different wall materials is achieved at almost similar values of  $V_L$ : -70 V for SS, -60 V for Al, and -50 for Cu. At optimized  $V_t$  and  $V_L$ , the values of  $H^-$  current density for Al, Cu, and SS are 0.01697, 0.01164, and 0.01085 mA/cm<sup>2</sup>, respectively.

For the case of aluminum, a 63% increase of  $H^-$  current density at optimum  $V_L$  is obtained compared with the extracted unfocused beam, clearly showing the focusing

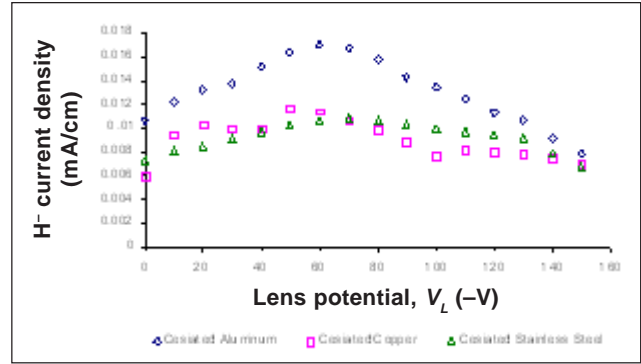


Fig. 5. Optimization of the focusing effect of the Einzel lens.

effect of the Einzel lens. The same enhancement in  $H^-$  yield is observed for copper (51%) and stainless steel (67%) at their corresponding optimum  $V_L$ .

The presented results from the plots above clearly indicate that the wall material of the ion source plays an important role in the production of  $H^-$  ions. Under the same discharge conditions, the performance of the different wall materials in terms of  $H^-$  yield differs significantly. From the plots, aluminum consistently generates the highest ion current, indicating that among the three it is the best metal liner for optimum beam extraction. Stainless steel, on the other hand, yields the lowest amount of ions, 64% lower than aluminum at optimum beam extraction parameters. This is consistent with the expected results based on the plasma parameter investigation since aluminum has the highest  $n_e$  and lowest  $T_e$  values. The first leads to a more efficient use of rovibrationally excited molecules, resulting in more negative ion formation (Bacal et al., 2002), and the second leads to less reduction of  $H^-$  within the plasma due to less impact processes with energetic or “hot” electrons that can contribute to neutralization of produced negative ions (Ramos et al., 1989).

The higher ion yield produced by aluminum is attributed to its lower work function as compared with stainless steel and copper. Aluminum’s work function  $f$  is only 4.28 eV, while Cu has  $f = 4.65$  eV. Stainless steel is approximately 65% iron ( $f = 4.7$  eV), 20% chromium ( $f = 4.5$  eV), and 10% nickel ( $f = 5.15$  eV). The work function of a material is the energy needed to remove an electron from the Fermi level in a metal to a point at infinite distance away outside the surface. The lower

the work function of the material is, the easier it would be to eject the electrons from the wall material into the bulk of the plasma. Bombardment by neutrals and ions along anode cusps would facilitate the removal of electrons. Within the plasma, the ejected electrons from the wall materials would contribute greatly to the formation of more  $H^-$  through the surface production process.

Additional reactions that generate  $H^-$  within the bulk of the plasma as described by the dissociative electron attachment process [Eqs. (1a) & (1b)] require the presence of low-energy electrons. The wall material of lower work function can contribute more electrons necessary for the aforementioned processes, yielding more  $H^-$ .

Thus, aside from the surface production process occurring at the Mo converter, additional  $H^-$  ions are produced at the walls and within the plasma.

Comparing the values of work functions of the metal liners and using the argument presented above, it is logical that the wall material that produces the most  $H^-$  is the aluminum liner as more electrons are easier to remove for electron dissociative electron attachment necessary for  $H^-$  production than from copper and stainless steel. The greater current obtained from the experiments agree well with this argument. Similarly, the almost identical values of the work functions of copper and stainless steel explain the comparable ion yield detected for the wall materials. Stainless steel, with the highest work function, yielded the least as expected. This also justifies why the yields of Cu and stainless steel overlap at certain plasma and beam conditions.

## CONCLUSION

Enhancement in the production of  $H^-$  may be achieved with proper selection of the wall material in the operation of the PSTIS. At optimum plasma parameters, results show that at 1.2 mTorr, aluminum generates the highest yield of 0.01697 mA/cm<sup>2</sup>, which is 64% more than the 0.01085 mA/cm<sup>2</sup> that stainless steel produces. The yield of copper, meanwhile, falls between the two materials at 0.011644 mA/cm<sup>2</sup>. The discrepancy in the metals' work functions accounts for the differences in the  $H^-$  yield among the wall materials. Aluminum having the lowest work function among the three yields the highest current.

## REFERENCES

- Bacal, M., et al., 2002. *Rev. Sci. Instrum.* **73**: 903.
- Fukumasa, O., et al., 1996. *Jpn. J. Appl. Phys.* **35**: L1528–31.
- Leung, K.N., K. W. Ehlers, & R. V. Pyle, 1985. *Appl. Phys. Lett.* **47**: 227.
- Nishiura, M., M. Sasao, & M. Wada, *Rev. Sci. Instrum.* **69**: 974.
- Ramos, H.J., et al., 1989. IPPJ-914 Research Report, Nagoya, Japan.
- Ramos, H.J., 1995. Development of negative ion sources for thin film formation. *Proceedings of the 15th Annual Conference of the Japan Society of Fusion and Plasma Science Research, Osaka.*
- Ranay, J.P., 2002. Investigation of plasma parameters for negative hydrogen ion extraction in a sputter-type negative ion source, B.S. thesis. National Institute of Physics, College of Science, University of the Philippines, Diliman.
- Ubarro, A.D., 2003. Effect of converter potential and Ar–H<sub>2</sub> mixing in the production of negative ions in a multicusp source, B.S. thesis. National Institute of Physics, College of Science, University of the Philippines, Diliman.
- Uramoto, J., 1985. IPPJ Research Report, Nagoya, Japan.
- Weast, R.C. (ed.), 1986. CRC handbook of chemistry and physics, 67th ed. CRC, Boca Raton, FL.
- Wengrow, A.B., et al., 1998. Development of a high duty factor, surface conversion  $H^-$  ion source for the LANSCE facility. *IEEE*.
- Yambot, M.L., 1999. Negative ion beam focusing study in a PSTNIS, B.S. thesis. National Institute of Physics, College of Science, University of the Philippines, Diliman.
- Yambot, M.L., 2003. Effect of cesium seeding on  $H^-$  ion production in a plasma sputter-type ion source, M.S. thesis. National Institute of Physics, College of Science, University of the Philippines, Diliman.